Clinical and Translational Imaging
https://doi.org/10.1007/s40336-024-00632-5

MINI REVIEW

Pediatric congenital pulmonary malformations: key findings at imaging

Giulia Fichera[1] · Annachiara Cavaliere[1] · Francesco Causin[1] · Monica Zuliani[1] · Gianni Bisogno[2] · Federico Rea[3] · Roberto Stramare[3] · Chiara Giraudo[3,4]

Received: 2 December 2023 / Accepted: 26 March 2024

Abstract
Pediatric congenital pulmonary malformations are rare abnormalities which may affect airways, pulmonary parenchyma, and vasculature and diagnostic imaging plays a significant role in their identification and characterization. Although, nowadays, often the diagnosis of this heterogeneous group of malformations is performed prenatally by ultrasound and/or fetal magnetic resonance, after birth, computed tomography represents the main technique. Radiographs are often used as first line diagnostic tool while magnetic resonance demonstrated to be especially beneficial to investigate some malformations such as bronchogenic cysts. Therefore, radiologists should be aware of the main features associated with such alterations to guarantee a prompt diagnosis and, if necessary, guide towards the optimal treatment. Aim of this pictorial review is to provide a comprehensive overview of the typical features of congenital pulmonary malformations at imaging supporting general and pediatric radiologists in the diagnostic process.

Keywords Children · Congenital malformations · Lung · Imaging

Introduction

Pediatric congenital pulmonary malformations (CPM) are rare abnormalities due to aberrant embryonic development and occurring from the prenatal stage to childhood [1, 2]. The most frequent malformations include congenital pulmonary airway malformation (CPAM), pulmonary sequestration, bronchogenic cyst, and congenital lobar overinflation [3].

Although CPM are often detected during prenatal ultrasound (US), an accurate characterization can be performed after birth by radiographs, computed tomography (CT), and Magnetic Resonance (MR) demonstrating the essential role of imaging. In fact, for instance, the localization and key radiological features, such as blind-ending bronchi at CT in children with aplasia, are crucial at diagnosis and guide the proper clinical and therapeutic management.

Thus, aim of this pictorial review is to provide to pediatric and general radiologists a comprehensive overview of the main characteristics and features at imaging of CPM subdivided according to the affected structure/s: (i) bronchopulmonary; (ii) vascular; (iii) and combined.

Bronchopulmonary malformations

Congenital pulmonary airways malformations

CPAM are subdivided into five classes (0–4) [4]: type 0 (1–3%), involves the trachea and the mainstem bronchi, being lethal in the postnatal stage; type I, (60–70%), affects the bronchi and the proximal bronchioles and it is associated with large cysts (2–10 cm); type II (15–20%) involves

✉ Chiara Giraudo
chiara.giraudo@unipd.it

1 Pediatric Radiology, University Hospital of Padova, Padova, Italy

2 Pediatric Hematology-Oncology Division, Department of Woman's and Child's Health, University Hospital of Padova, Padova, Italy

3 Unit of Thoracic Surgery, Department of Cardiac, Thoracic, Vascular Sciences and Public Health – DCTV, University of Padova, Padova, Italy

4 Unit of Advanced Clinical and Translational Imaging, Department of Cardiac, Thoracic, Vascular Sciences and Public Health – DCTV, University of Padova, Via Giustiniani 2, Padova, Italy

Published online: 02 April 2024

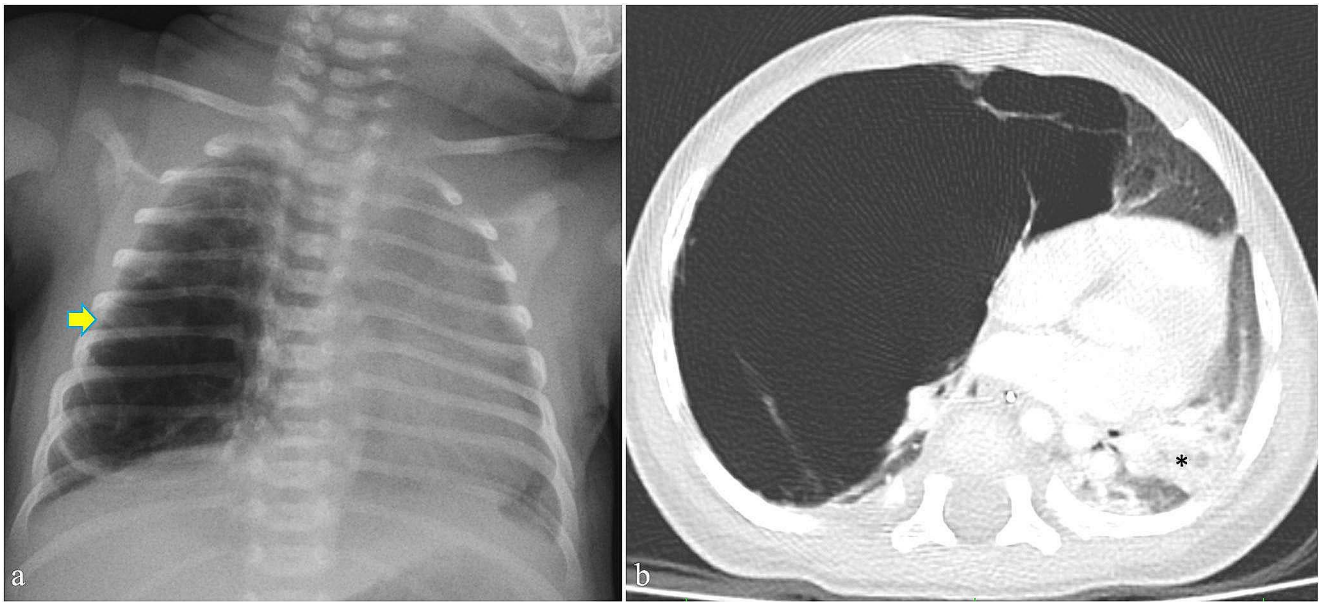

Fig. 1 Six-month-old infant with hyperlucencies of the right lung (yellow arrow in a) and mediastinal shift on the left side at chest X-ray. The chest computed tomography in b shows a large cyst on the right side due to congenital pulmonary airway malformation (CPAM) type 1, confirms the left mediastinal shift and demonstrates partial atelectasis of the left lower lobe (black asterisk in b)

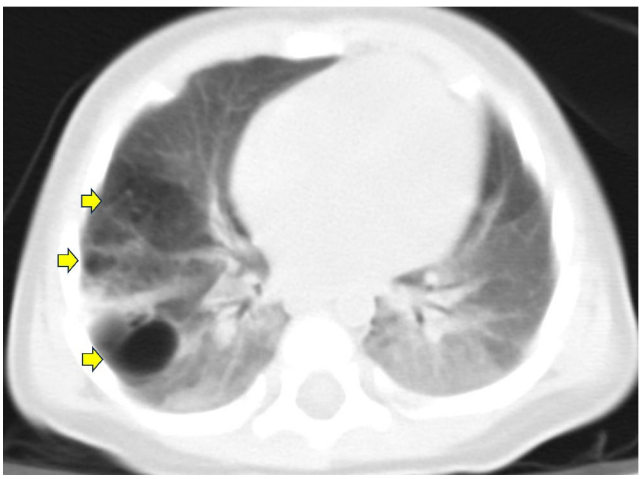

Fig. 2 Axial chest computed tomography of a 3-month-old infant demonstrating cysts smaller than 2 cm in the right lung due to congenital pulmonary airway malformation (CPAM) type II.

the bronchiolar area with cysts of less than 2 cm; type III (10%) affects the bronchiolar/alveolar duct region while type IV (5–10%) involves the alveolar/saccular region causing unlined cysts. Type I and II cysts can be easily seen as lucencies, often associated with mediastinal shift, on radiographs. CT allows a better characterization of cyst size, enables the detection of small cysts (type II) (Figs. 1 and 2) and the identification of associated cardiac (type I) and renal (type II) malformations. The microcysts typical of type III may appear as a homogeneous hypodense mass at CT. Last, imaging is not accurate in assessing type IV since it is almost indistinguishable from type I [5, 6]. The proximal airways communication and the vascular supply of CPAM allows the differentiation from pulmonary sequestration [5].

Tip: usually unilateral single or multiple cystic lesions and in the neonatal period, the cysts may be fluid-filled and therefore show air-fluid levels or seem solid.

Agenesia-aplasia-hypoplasia complex

The pulmonary underdevelopment complex is classified into three types [5]: agenesis (type I), complete absence of bronchopulmonary and vascular structures; aplasia (type II), absence of lung parenchyma with a blind-ending bronchus; and hypoplasia (type III), reduced number of airways and vessels [5]. Radiographs of agenesis show unilateral diffuse pulmonary opacification, ipsilateral mediastinal shift, and contralateral lung hyperinflation while CT is more accurate in identifying the missing parenchyma, bronchial branches, and pulmonary artery [5] (Fig. 3). Aplasia has similar features at imaging but in addition a blind-ending pouch at the end of the bronchus can be seen. Asymmetrically small lungs with narrowed bronchi are typical of hypoplasia [7].

Tip: it is usually associated with malformations in other systems such as the gastrointestinal, cardiovascular, genitourinary, and skeletal ones.

Congenital lobar overinflation

Congenital lobar overinflation is idiopathic in around 50% of the cases while defective bronchial cartilages causing bronchial collapse and air-trapping in expiration affects

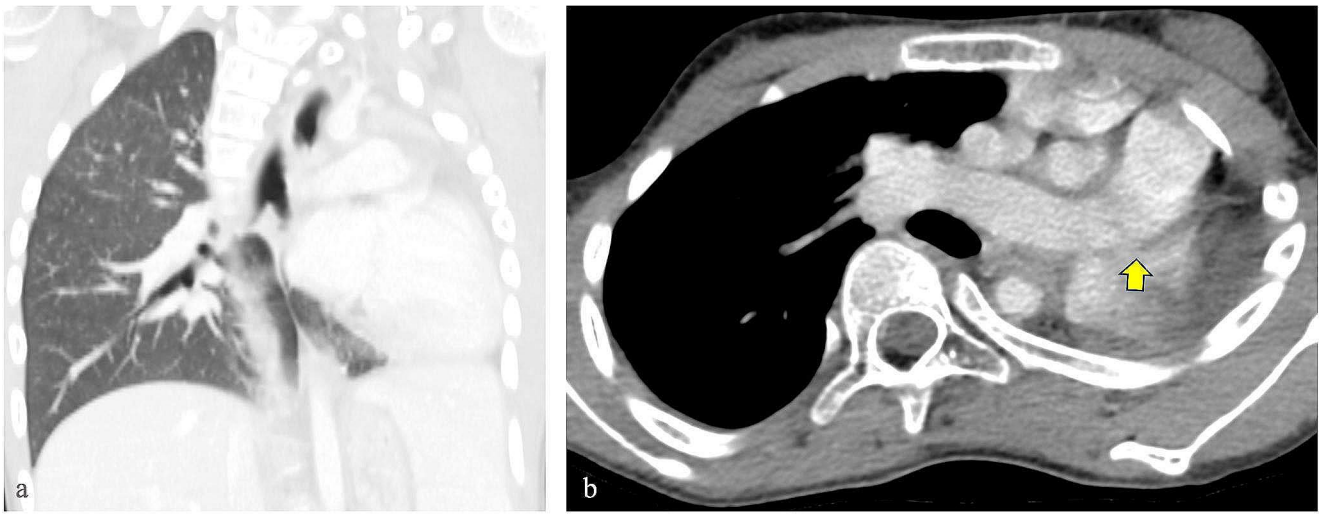

Fig. 3 In a, lung window coronal reconstruction of the computed tomography of a 10-year-old girl with agenesia of the left upper lobe and mediastinal shift (a); in b, axial mediastinal window showing the agenesia of the left main pulmonary artery (yellow arrow)

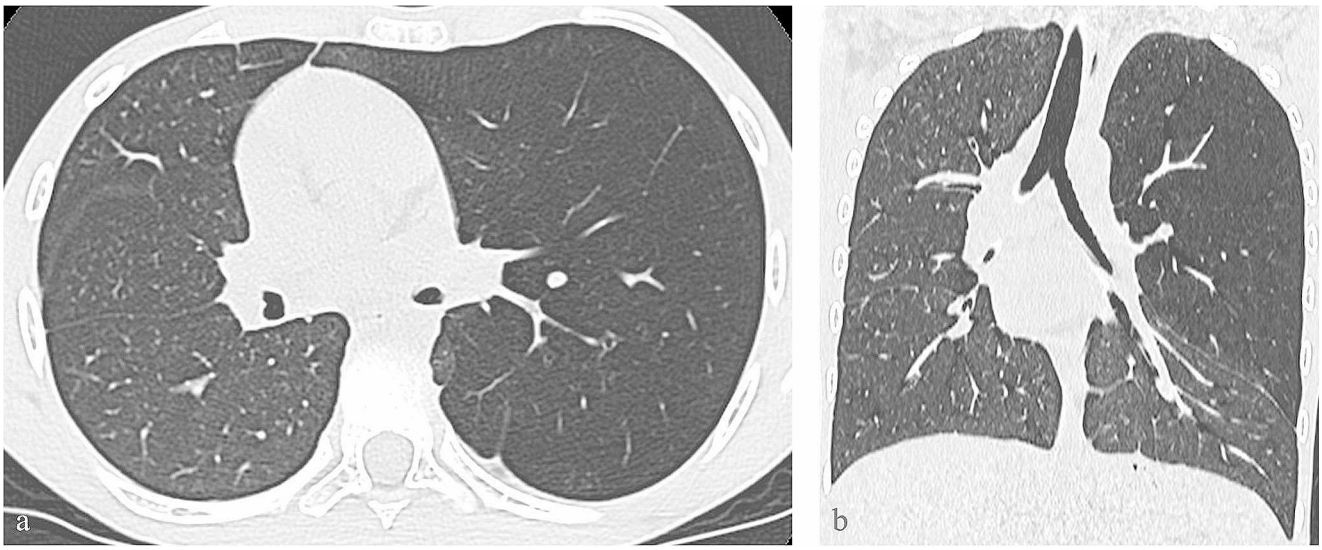

Fig. 4 Nine-year-old boy with congenital overinflation of the upper left lobe (axial and coronal computed tomography images in a and b, respectively)

25% of the patients [8]. The upper left lobe is most frequently involved followed by the middle lobe. Overinflation, lucency, and contralateral mediastinal shift are evident at radiographs. CT is more accurate also for the detection of compression or atelectasis of the surrounding parenchyma [9, 10] (Fig. 4).

Tip: it can be associated with pulmonary sling (*see below*) and congenital heart defects.

Congenital tracheal malformations

Various tracheal anomalies including tracheomalacia, accessory bronchi, and diverticula may occur and can be nicely assessed by CT taking advantage of 3D reconstructions.

Tracheomalacia is seen at CT as a loss of the usual tracheal semicircular shape [11, 12]. Dilatation of the trachea (> 3 cm) on the inspiratory phase and its crescent shape (antero-posterior diameter < 50% or more) during expiration may support the diagnosis [13].

The most frequent accessory bronchi are the tracheal bronchus (aka pig bronchus), usually originating 2–6 cm proximal to the carina, and the cardiac bronchus that arises from the bronchus for the right upper lobe and is blind-ended [14] (Fig. 5).

These anatomical variants are usually asymptomatic, and the diagnosis is incidental although patients may experience infections, plugs, stridor, or even foreign body aspiration [14].

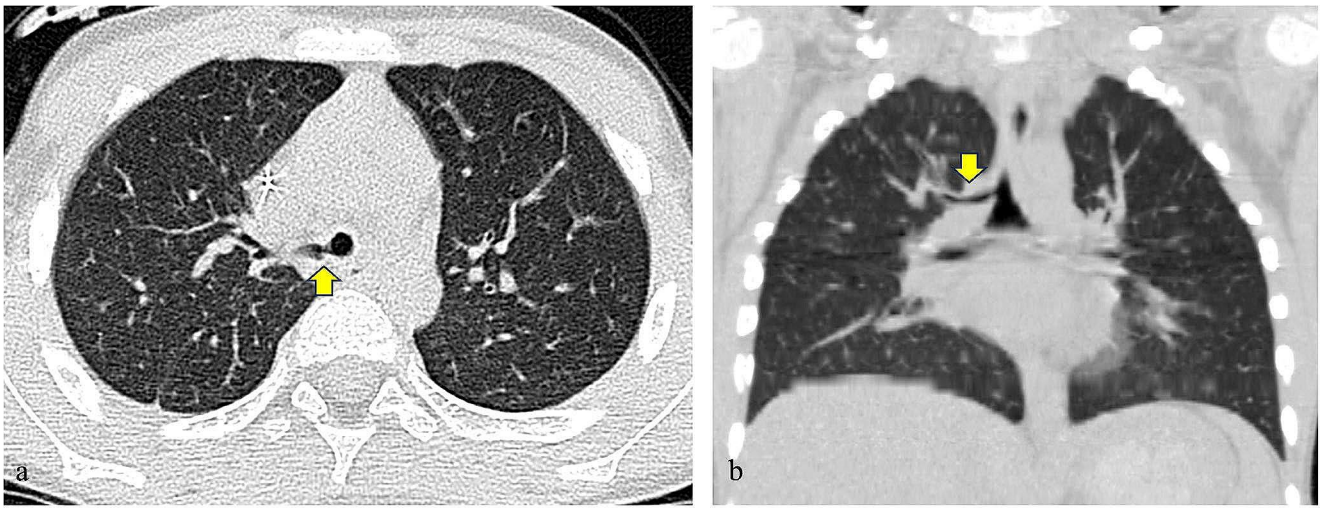

Fig. 5 Six-year-old boy with right tracheal bronchus (aka pig bronchus) nicely seen on the axial and coronal computed tomography images (yellow arrow in a and b, respectively)

Fig. 6 Axial CT of a 17-year-old girl showing a small tracheal diverticulum on the right side (yellow arrow)

Tracheal diverticula are single or multiple pouches often located on the right posterolateral wall of the trachea at CT (Fig. 6) [15].

Tip: they should be suspected in children with respiratory distress and retraction as well as repeated respiratory infections while dyspnea can be episodic.

Bronchogenic cyst

Bronchogenic cysts are foregut-derived cystic malformations of the respiratory tract located in the middle mediastinum or in the lungs [16]. Radiographs may show well-defined rounded opacities or air-fluid cavities. Mediastinal lesions might be overlooked unless causing a focal enlargement of the mediastinal lines.

At CT round hypo-/hyperdense malformations containing air-fluid levels and/or calcifications can be seen [7] (Fig. 7a). MR is useful for the characterization of the cyst which can express variable signal on T1w according to the protein content [17, 18] (Fig. 7b and c).

Tip: it is often asymptomatic and therefore diagnosed as incidental finding; it may become symptomatic if very large, then causing bronchial obstruction, or infected.

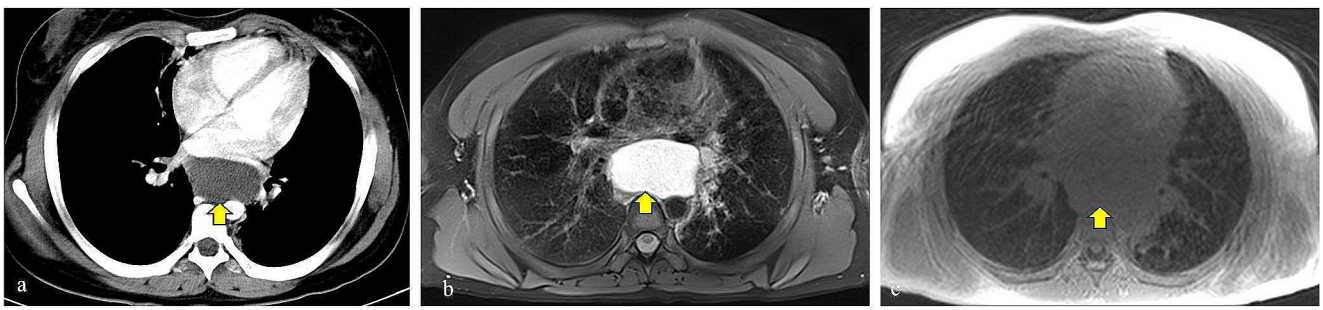

Fig. 7 Axial chest computed tomography with contrast medium of a 17-year-old girl nicely showing a mediastinal bronchial cyst (yellow arrow in a). The same patient underwent a follow-up by magnetic resonance ten years later which showed stable dimensions of the lesion and confirmed its homogeneous fluid content (hyperintense on the axial T2weighted blade fat-saturated in b and hypointense on the 3D T1weighted volumetric interpolated breath-hold examination (VIBE) in c)

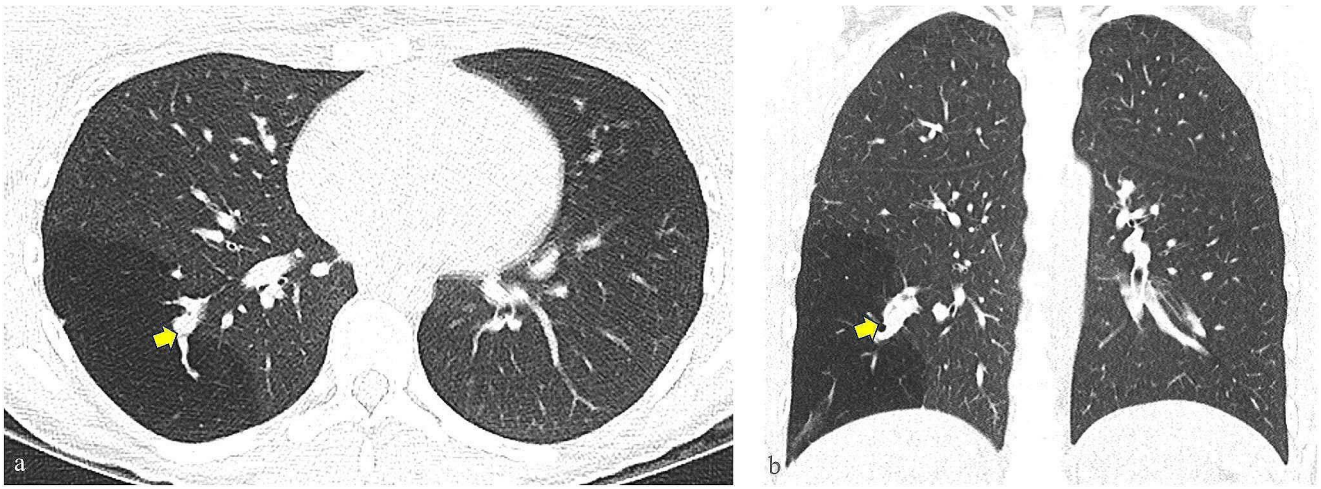

Fig. 8 Axial (a) and coronal (b) CT images of a 17-year-old girl showing a bronchocele (yellow arrow in a and b) and hyperinflation of the adjacent lung parenchyma, signs of bronchial atresia

Bronchial atresia

Bronchial atresia is the obliteration of the proximal part of a bronchus [19]. It usually occurs in the apico-posterior segmental bronchus. Radiographs may show hilar round opacities and distal pulmonary hyperlucencies. A recent study on adults and children demonstrated that it can be easily diagnosed by CT, identifying a bronchocele with hyperinflation of the adjacent lung parenchyma [20] (Fig. 8).

Tip: it is usually an incidental finding, but it may cause recurrent infections.

Vascular anomalies

Vascular anomalies can be divided into three groups according to the type of involved vessels [10].

Anomalies of the pulmonary artery

The absence of the pulmonary artery is a rare condition resembling pulmonary aplasia and hypoplasia on radiographs. Indeed, lung volume loss, mediastinal shift, and compensatory hyperinflation are the main signs. At CT interlobular septal thickening and small cystic changes can be seen [10].

The abnormal origin of the left pulmonary artery from the right side (aka pulmonary sling) is very rare and is probably due to the obliteration of the left sixth aortic arch [10]. On radiographs, a right paratracheal mass and ipsilateral lung hyperinflation due to compression of the right main bronchus may occur [10]. CT angiography including 3D reconstruction is the modality of choice to characterize this vascular anomaly [21].

Fig. 9 Sagittal steady state free precession magnetic resonance image showing the enlarged inferior right vein (white arrow) draining into the inferior vena cava (black asterisk)

Tip: respiratory distress usually starts in the early neonatal phase.

Pulmonary venous drainage anomalies

Total or partial anomalous pulmonary venous connection or return (TAPVR and PAPVR, respectively) include a large spectrum of cardiovascular malformations with pulmonary veins returning to the right atrium or systemic venous circulation instead of draining into the left atrium.

TAPVR usually causes neonatal cyanosis while children with PAPVR can be asymptomatic. CT and MR angiography nicely show the vascular anomalies [10] (Figs. 9 and 10).

Fig. 10 Contrast-enhanced magnetic resonance-angiography showing the anomalous drain of three right pulmonary veins (vv) in the superior vena cava (svc)

Tip: over time the left-to-right shunt in PAPVR may cause pulmonary hypertension and in the long run it may reverse in right-to-left shunt with systemic cyanosis and Eisenmenger's syndrome.

Pulmonary arteriovenous malformation

Pulmonary arteriovenous malformation are classified in three types: (i) simple, the most frequent, with a single segmental artery feeding; (ii) complex, with multiple feeding segmental arteries; (iii) diffuse, with hundreds of malformations [22]. Radiographs may show unilateral, nodular, and curvilinear opacities but contrast-enhanced CT and MR allow the detection of the feeding vessels [10] (Fig. 11).

Tip: they are usually asymptomatic but dyspnea and embolic events may occur.

Combined pulmonary and vascular anomalies

Pulmonary sequestration

Pulmonary sequestration is due to a segment or lobe without communication with the tracheobronchial tree and receiving anomalous vascular supply [23].

Intralobar sequestration occurs within the visceral pleura of the functioning lung, the venous drainage is into the pulmonary vein and it is often reported in the left lower lobe. Extralobar sequestration has separate visceral pleura and venous drainage into the systemic veins. Arterial supply from the descending thoracic aorta is typical and can be easily detected at imaging. Indeed, it can be seen by US in the prenatal phase as hyperechoic mass or by fetal MR as hyperintense lesion on T2-weighted images (Fig. 12). In the post-natal phase, contrast enhanced CT or MR are applied to confirm the findings [5] (Fig. 13).

Tip: it is commonly associated with recurrent pneumonia; cough, exertional dyspnea, and hemoptysis may occur.

Scimitar syndrome

The scimitar syndrome is a PAPVR variant resulting in a left-to-right shunt [5]. At radiographs the anomalous draining vein can be seen as a tubular structure running parallel

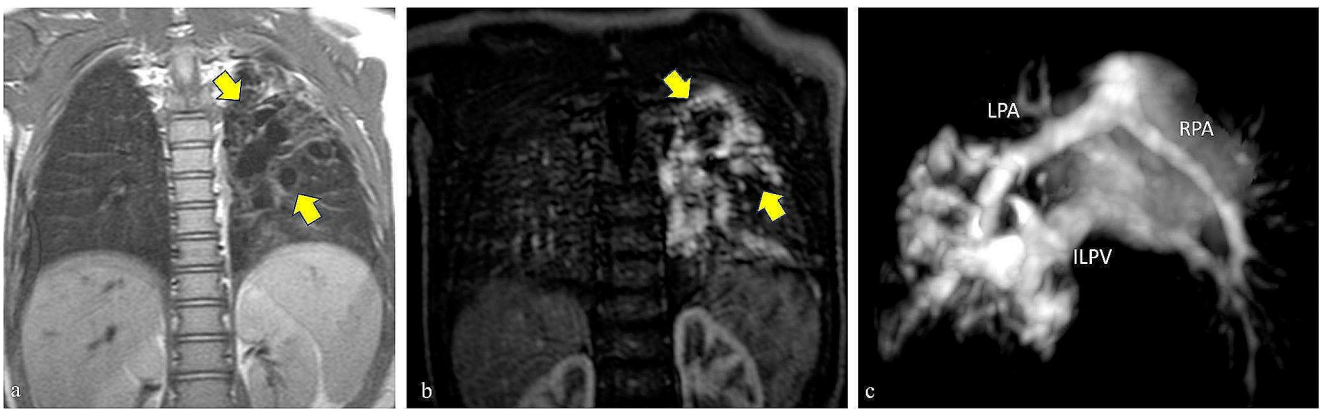

Fig. 11 Coronal proton density showing the flow voids in the left lung due to a vascular malformation (in a), coronal post-contrast 3D cine SENSE (Enhanced sensitivity encoding in b) showing the vascular enhancement, and 3D reconstruction (in c) nicely demonstrating the vascular supply (LPA, left pulmonary artery, RPA, right pulmonary artery, ILPV, inferior left pulmonary vein)

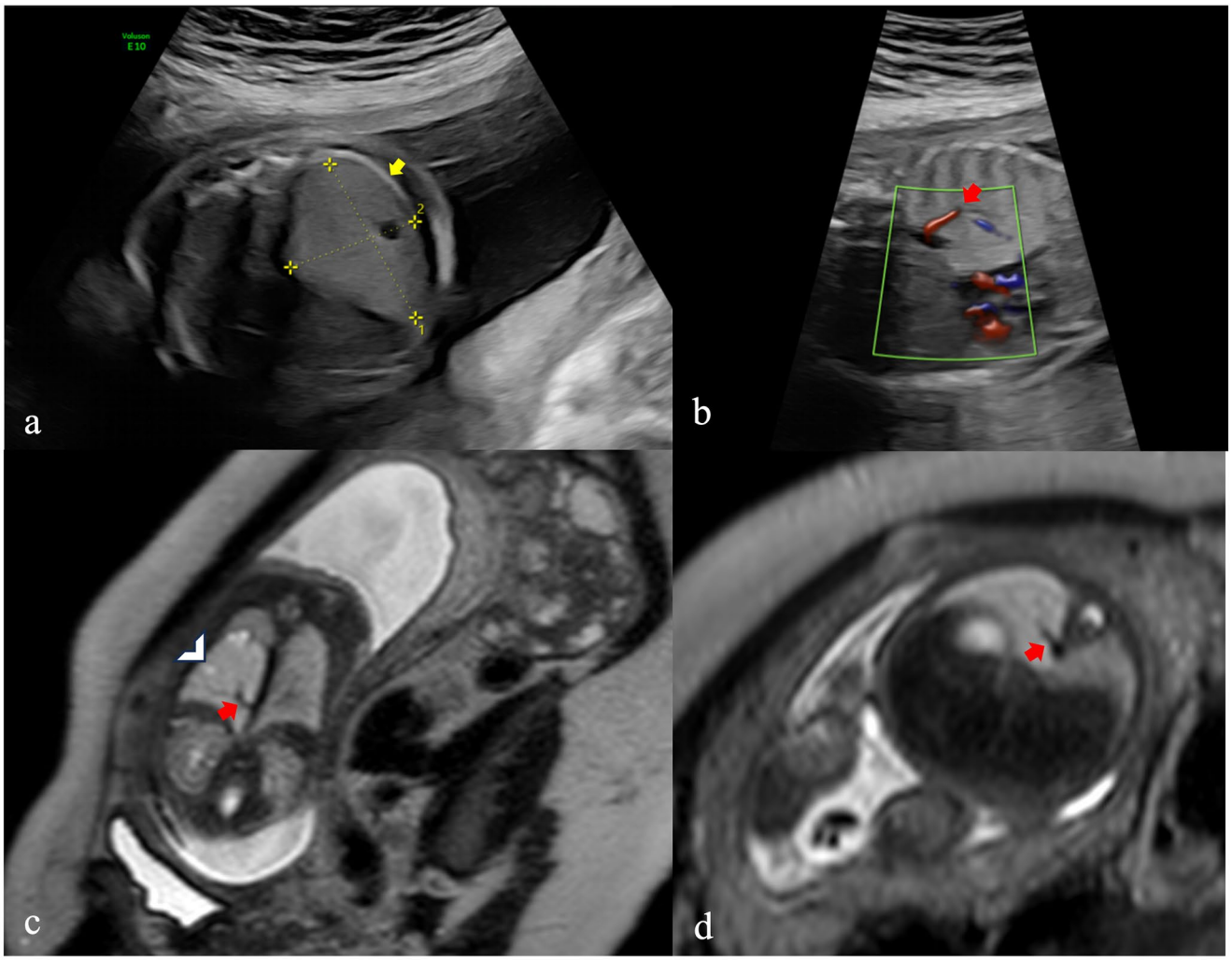

Fig. 12 Prenatal US images of a fetal lungs at 25 weeks of gestation demonstrating a pulmonary hyperechoic lesion on the right side (yellow arrow in a) with abnormal blood vessel at Power Doppler image (red arrow in b), due to pulmonary sequestration. The fetal magnetic resonance (MR) performed 26 weeks after gestation confirmed the diagnosis as demonstrated by the hyperintense area on the coronal T2-weighted MR image (white arrowhead in c) with abnormal vascular supply from the aorta (red arrow in c and in d)

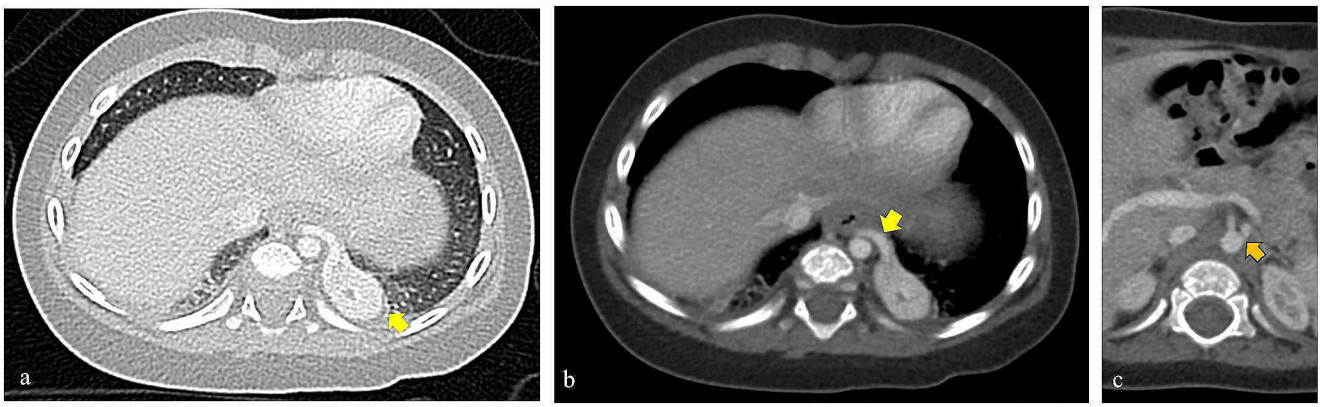

Fig. 13 Ten-month-old girl with aberrant segmental lung tissue in the left lower lobe without any connection to the tracheobronchial tree (yellow arrow in a and b) receiving vascular supply from a branch of the descending aorta (orange arrow in c), typical findings of intralobar pulmonary sequestration

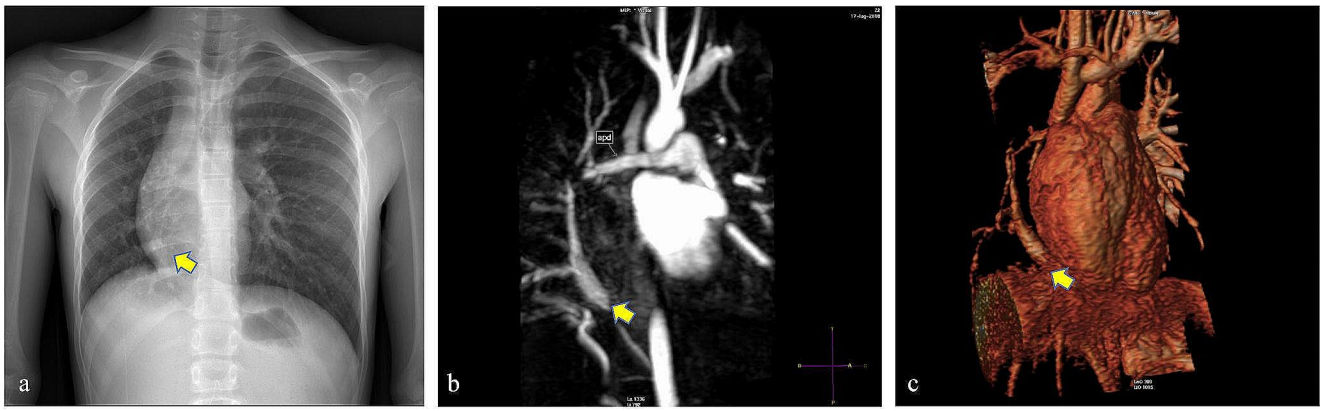

Fig. 14 Eleven years-old female with fatigue who underwent chest x-ray showing a tubular structure running parallel to the right heart margin, recalling the shape of a Turkish sword (yellow arrow in a). Fat Saturated T2-weighted and 3D reconstruction images (yellow arrow in b and c) well demonstrating the anomalous draining vein confirming the Scimitar syndrome

to the right cardiac chambers, recalling the shape of a Turkish sword. Contrast-enhanced CT and MR well demonstrate the "scimitar" vein drainage into the inferior vena cava, the hypoplastic right lung, and the associated anomalies [5] (Figs. 14 and 15).

Tip: it may be associated with congenital cardiovascular defects as well as anomalies in other organs.

Conclusions

Pediatric pulmonary malformations are rare and complex anomalies which can be well characterized by imaging. Radiologists should be aware of their main characteristics to guarantee a correct diagnosis and then properly guide the clinicians towards the optimal therapeutic management.

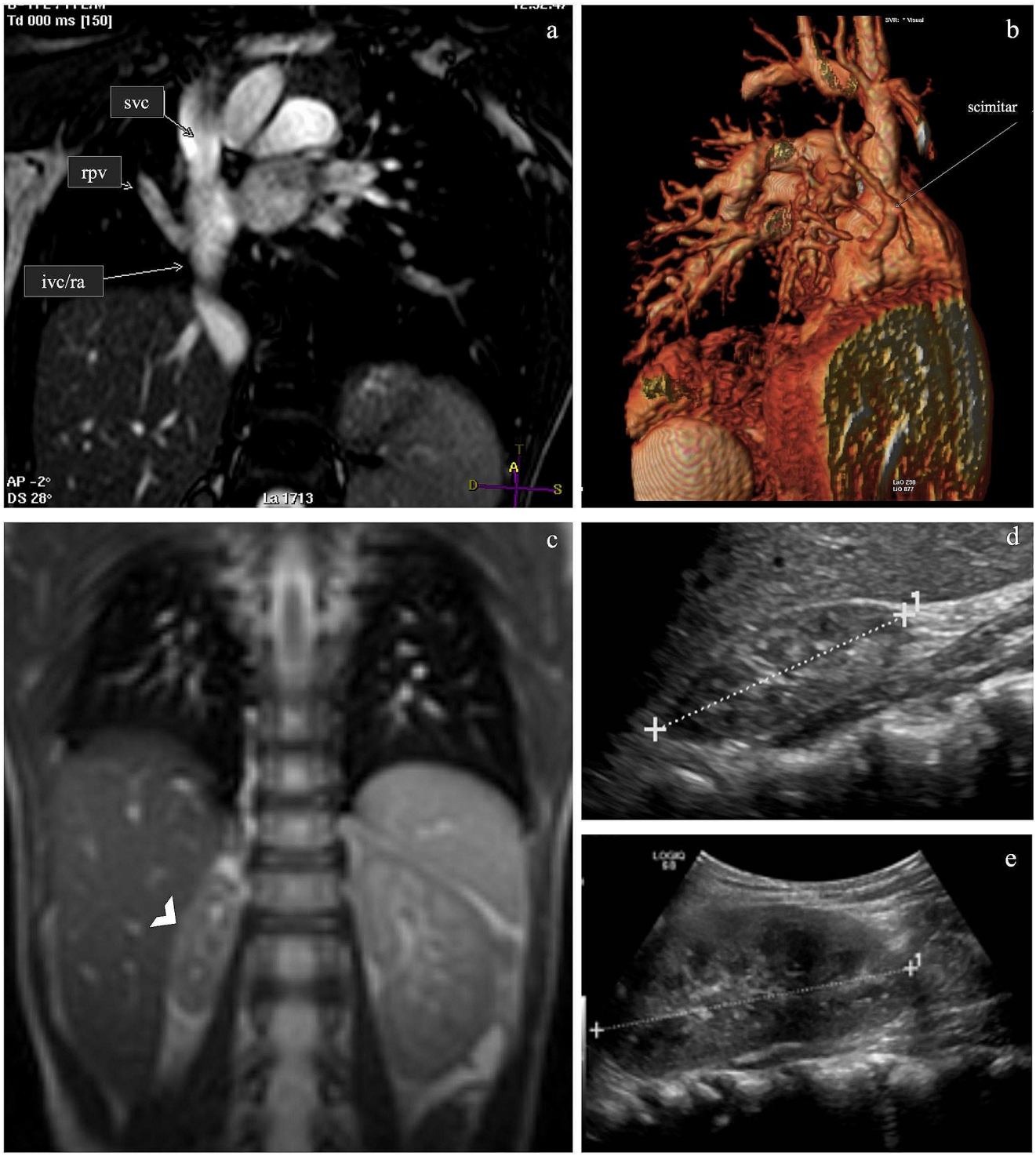

Fig. 15 Five years-old boy with scimitar syndrome as demonstrated by the multiplanar and 3D post-contrast MR reconstruction (a and b; ivc: inferior vena cava; ra: right artery; rpv: right pulmonary vein; svc: superior vena cava) associated with right renal hypoplasia (arrow head on the coronal MR in c and ultrasound in d). In e the ultrasound image of the left regular kidney

Author contributions Conceptualisation: G.F. and C.G. Writing - original draft preparation: G.F. and A.C. Figure preparation: G.F., A.C., M.Z. Resources: F.C., F.R., R.S. Writing— review and editing: A.C., F.C., G.B., M.Z., F.R., R.S., C.G. Supervision: C.G. All authors contributed to the article and approved the submitted version.

Funding Open access funding provided by Università degli Studi di Padova within the CRUI-CARE Agreement.

Data availability No datasets were generated or analysed during the current study.

Declarations

Competing interests The authors declare no competing interests.

References

1. Nadeem M, Elnazir B, Greally P (2012) Congenital pulmonary malformation in children. Scientifica. 209896
2. Caldeira I, Fernandes-Silva H, Machado-Costa D, Correia-Pinto J, Moura RS (2021) Developmental pathways underlying Lung Development and congenital Lung disorders. Cells 10:2987
3. Carsin A, Mely L, Chrestian MA, Devred P, de Lagausie P, Guys JM, Dubus JC (2010) Association of three different congenital malformations in a same pulmonary lobe in a 5-year-old girl. Pediatr Pulmonol 45:832–835. https://doi.org/10.1002/ppul.21068
4. Yikilmaz A, Lee EY (2007) CT imaging of mass-like nonvascular pulmonary lesions in children. Pediatr Radiol 37:1253–1263. https://doi.org/10.1007/s00247-007-0637-4
5. Biyyam DR, Chapman T, Ferguson MR, Deutsch G, Dighe MK (2010) Congenital lung abnormalities: embryologic features, prenatal diagnosis, and postnatal radiologic-pathologic correlation. Radiographics 30:1721–1738. https://doi.org/10.1148/rg.306105508
6. Shimohira M, Hara M, Kitase M, Takeuchi M, Shibamoto Y, Kurono K, Shimizu S (2007) Congenital pulmonary airway malformation: CT-pathologic correlation. J Thorac Imaging 22:149–153. https://doi.org/10.1097/01.rti.0000213586.06602.d3
7. Daltro P, Fricke BL, Kuroki I, Domingues R, Donnelly LF (2004) CT of congenital lung lesions in pediatric patients. AJR Am J Roentgenol 183:1497–1506
8. Mukhtar S, Trovela DAV (2022) Congenital Lobar Emphysema. In: StatPearls. Treasure Island (FL). In: StatPearls [Internet]. Treasure Island (FL): StatPearls Publishing; 2023 Jan-. https://www.ncbi.nlm.nih.gov/books/NBK560602/
9. Lee EY, Boiselle PM, Cleveland RH (2008) Multidetector CT evaluation of congenital lung anomalies. Radiology 247:632–648. https://doi.org/10.1148/radiol.2473062124
10. Cherian SV, Kumar A, Ocazionez D, Estrada-Y-Martin RM, Restrepo CS (2019) Developmental lung anomalies in adults: a pictorial review. Respir Med 155:86–96. https://doi.org/10.1016/j.rmed.2019.07.011
11. Boogaard R, Huijsmans SH, Pijnenburg MW, Tiddens HA, de Jongste JC, Merkus PJ (2005) Tracheomalacia and bronchomalacia in children: incidence and patient characteristics. Chest 128:3391–3397. https://doi.org/10.1378/chest.128.5.3391
12. Hysinger EB, Bates AJ, Higano NS, Benscoter D, Fleck RJ, Hart CK, Burg G, De Alarcon A, Kingma PS, Woods JC (2020) Ultrashort Echo-Time MRI for the Assessment of Tracheomalacia in neonates. Chest 157:595–602
13. Boiselle PM, Lee KS, Lin S, Raptopoulos V (2006) Cine CT during coughing for assessment of tracheomalacia: preliminary experience with 64-MDCT. AJR Am J Roentgenol 187:W175–177
14. Ulusoy M, Kıvrak AS, Uysal II, Karabulut AK, Paksoy Y, Fazlıogulları Z (2013) Developmental anomalies of bronchial tree: a Multidetector Computerized Tomography Study. Int J Morphol 31:1049–1055
15. Lin H, Cao Z, Ye Q (2014) Tracheal diverticulum: a case report and literature review. Am J Otolaryngol 35:542–545. https://doi.org/10.1016/j.amjoto.2014.03.015
16. Limaïem F, Ayadi-Kaddour A, Djilani H, Kilani T, El Mezni F (2008) Pulmonary and mediastinal bronchogenic cysts: a clinicopathologic study of 33 cases. Lung 186:55–61
17. Nakata H, Egashira K, Watanabe H et al (1993) MRI of bronchogenic cysts. J Comput Assist Tomogr 17:267–270. https://doi.org/10.1097/00004728-199303000-00016
18. Limaiem F, Mlika M, Bronchogenic Cyst [Updated 2023 Jul 4]. In: StatPearls [Internet]. Treasure Island (FL): StatPearls Publishing; 2023 Jan-. https://www.ncbi.nlm.nih.gov/books/NBK536973/
19. Hutchison MJ, Winkler L (2023) Bronchial atresia. StatPearls. Treasure Island (FL), vol 26. StatPearls Publishing
20. Puglia EBMD, Rodrigues RS, Daltro PA, Souza AS Jr, Paschoal MM, Labrunie EM, Irion KL, Hochhegger B, Zanetti G, Marchiori E (2021) Tomographic findings in bronchial atresia. Radiologia Brasileira 54:9–14. https://doi.org/10.1590/0100-3984.2019.0136
21. Leonardi B, Secinaro A, Cutrera R et al (2015) Imaging modalities in children with vascular ring and pulmonary artery sling. Pediatr Pulmonol 50:781–788. https://doi.org/10.1002/ppul.23075
22. Meek ME, Meek JC, Beheshti MV (2011) Management of pulmonary arteriovenous malformations. Semin Intervent Radiol 28:24–31. https://doi.org/10.1055/s-0031-1273937
23. Ko SF, Ng SH, Lee TY, Wan YL, Liang CD, Lin JW, Chen WJ, Hsieh MJ (2000) Noninvasive imaging of bronchopulmonary sequestration. Am J Roentgenol 175:1005–1012